Tribology International 155 (2021) 106789

Contents lists available at ScienceDirect

Tribology International

journal homepage: http://www.elsevier.com/locate/triboint

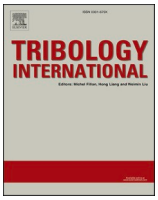

Understanding the generation of wear particles in cold rolling processes

M.A. Mekicha [a,*], M.B. de Rooij [a], L. Jacobs [a,b], D.T.A. Matthews [a,b], D.J. Schipper [a]

[a] Department of Mechanics of Solids, Surfaces & Systems (MS^3), Faculty of Engineering Technology, University of Twente, Enschede, the Netherlands
[b] Tata Steel, Research & Development, IJmuiden, the Netherlands

ARTICLE INFO

Keywords:
Wear modelling
Scratch experiment
Wear particle size
Surface cleanliness

ABSTRACT

In this paper, the influence of rolling parameters on the generation of wear particles is studied experimentally using a pilot scale rolling mill. Further, a multi-scale wear model is proposed to predict the amount of wear particles generated in cold rolling processes operating under the boundary lubrication. Rolling experiments revealed that thickness reduction and roll roughness are the two dominant process parameters that control wear particles generation in cold rolling processes. Analysis of the wear particles size distribution showed that most of the wear particles are less than 5 μm in diameter. The proposed model captures the trend correctly and give values in the same order of magnitude as the experiments in terms of the volume of wear particles generated.

1. Introduction

High surface quality is desired for cold rolled sheet metals, particularly for applications in the automotive sector (e.g. outer body parts) and packaging sector (e.g. food and beverage cans). Surface cleanliness, which can be defined as the absence of undesirable material on the surface, is one measure of the surface quality of a cold rolled sheet metal. A cold rolled sheet metal with poor surface cleanliness can have a negative impact on the final product as well as adversely affect subsequent processes such as annealing, galvanizing and forming. For example, it can cause extreme dross inclusions and/or locally weakened zinc coating in hot dip galvanizing lines [1,2]. One of the key factors that decrease sheet metal (strip) cleanness are wear particles, which are generated during cold rolling due to the relative sliding of the roll and the strip in the roll bite [3,4]. The roll-strip contact in cold rolling is illustrated in Fig. 1a. The strip metal is drawn into the roll bite by the exit tension and the frictional force between the roll and the strip. The relative speed between the roll and the strip surface varies throughout the roll bite. The peripheral speed of the rolls and the speed of the strip are equal only at the neutral point. The roll moves faster than the strip before the neutral point, whereas the strip moves faster than the roll after the neutral point, as illustrated in Fig. 1b. In other words, the roll moves forward and backward relative to the strip before and after the neutral point, respectively. As a result, the roughness peaks of the much harder roll plough through the soft strip material being rolled. This leads to the formation of wear particles, which originate mainly from the sheet being rolled [2,5].

Increasing demands in higher surface quality of cold rolled sheet metals requires increased understanding and control of wear debris formation. The whole cold rolling tribological system, which involves a dynamic interaction of the rolls, the sheet metal and the lubricant/coolant, governs the sheet surface cleanliness. Process parameters (such as rolling pressure, pass reduction and rolling speed) as well as the surface roughness of the rolls and the sheet, material properties, surface treatment of the rolls (coated or not), and lubricant type and composition control the tribological behavior and the total amount of wear particles generated. Therefore, a thorough understanding of the rolling tribological system and the main process parameters that influence wear particles generation is crucial to control and tailor the surface cleanliness of a cold rolled sheet metal.

Many experimental studies have been conducted to investigate the wear mechanism and the influence of rolling parameters on the rate of wear particles formation in cold rolling processes. Jacobs et al. [2,3] carried out extensive rolling experiments on pilot rolling mills and studied the origin and composition of wear particles. Moreover, they studied the influence of roll roughness, Cr plating the rolls, thickness, rolling speed, incoming strip temperature and lubricant composition on strip cleanliness. Dubar and co-workers developed a laboratory experimental setup to simulate cold rolling contact conditions and investigated the influence of several rolling parameters such as thickness reduction and stress reversal [6], roughness and lubricant entrapment [7,8], interface temperature [8], and forward slip [6,8] on wear particles formation. Labiapari et al. [5] performed laboratory cold rolling experiments and investigated the influence of thickness reduction ratio,

* Corresponding author.
E-mail address: m.a.mekicha@utwente.nl (M.A. Mekicha).

https://doi.org/10.1016/j.triboint.2020.106789
Received 18 September 2020; Received in revised form 16 November 2020; Accepted 22 November 2020
Available online 26 November 2020

lubricant temperature as well as the hardness, previous annealing and surface finish of the sheet on the formation of wear debris in stainless steel cold rolling.

Although these studies provide an insight on the influence of rolling parameters on the rate of wear particles formation, little or no attempt has been made to develop a wear model for cold rolling processes to estimate the amount of wear particles generated. The dynamic and complex nature of cold rolling with many interacting variables makes it very challenging to develop a wear model. Huart et al. [7] attempted to relate the rate of wear particles formation to the accumulated plastic strain energy in the strip asperities by modelling the plastic behavior of the (strip) asperities using two dimensional finite element method (FEM) simulations in the case of a rigid smooth roll and a deforming rough strip. However, developing a wear model for cold rolling processes has the prerequisite that the macroscale rolling parameters that define the contact conditions at the microscale as well as the microscale wear mechanism at asperity level are both taken into account.

It has been repeatedly shown in literature [2,9–12] that abrasive wear is the dominant wear mechanism and is the main cause of wear particles formation in lubricated cold rolling processes. The total amount of wear particles generated due to abrasive wear in lubricated contacts depends on the real contact area, the geometry of the microscale contacting asperities, the sliding distance, lubricant and material properties, and surface treatment of the interacting surfaces. In cold rolling, the rolling force, thickness reduction and forward slip define the real contact area and the sliding distance. The roughness of the rolls and the strip determine the geometry of the microscale contacting asperities. The strip material, pretreatment of the strip and the rolls (e.g. pickling and coating respectively), roll material and hardness, temperature, and lubricant composition collectively determine the (degree and type of) wear at each micro-contact. Thus, any model that attempts to estimate the rate of wear particles formation in cold rolling should take into account the rolling parameters that have the most influence on the wear debris formation.

In this paper, a multi-scale wear model is proposed to predict the severity of wear particles generation due to abrasive wear for cold rolling processes operating under boundary lubrication. Boundary lubrication corresponds to the lubrication regime in the first stand of a tandem cold rolling mill, which has been empirically observed to be a stand where most of the wear particles are formed. It is therefore of most relevance. The film thickness parameter, for typical first stand rolling conditions, was calculated to be between 0.1 and 0.15 using Wilson and Walowit's equation [13]. In addition to operating in the boundary lubrication regime, this stand is where the largest thickness reduction occurs. High thickness reduction means harsher contact conditions, with high contact stresses and increased contact area and slip, which leads to more wear. Moreover, the typical input strip in this stand is soft (hot rolled and pickled) and has very irregular surface roughness features created by pickling. The proposed wear model combines a semi-analytical deterministic multi-asperity contact model and wear at microscale single asperity contact. Furthermore, cold rolling experiments were conducted, using a semi-industrial cold rolling pilot mill, to study the influence of rolling parameters on wear particles formation. The rolling experiments were done at several combinations of roll roughness, lubrication condition, rolling speed and exit tension. Finally, the model results are compared with the experimental measurements.

2. Computational procedure

The flow diagram of the proposed wear model is illustrated in Fig. 2. The inputs to the model are the three-dimensional (3D) strip and roll roughness topography (obtained using confocal microscopy measurements), constitutive equation of the strip material, thickness reduction, rolling speed, forward slip, and entry and exit tension. First, the real area of contact between the roll and the strip surface is calculated by employing a fully plastic contact model, in which the real contact area due to normal loading and bulk deformation of the strip are taken into account. The roll is assumed to be rigid and the strip as rigid-plastic. The details of the contact model and its experimental validation can be found in our previous publication [14]. The mean contact pressure, which is an input to the contact model, is determined from the friction hill calculations made using slab analysis under plane strain conditions [15]. In the friction hill calculations, the rolling force, contact pressure distribution, relative velocity between the roll and the strip, length of arc of contact, and bite angle are determined. The outputs of the contact model are the real contact area ratio, identification of the micro contacts and the surface finish of the rolled strip. Note that the real contact area varies throughout the roll bite as the bulk strain and the contact pressure vary across the roll bite. However, for simplicity and computational speed, the real contact area at the roll bite exit is used for wear calculations. This may lead to a slight overestimation of the real contact area, and consequently, the amount of wear particle generated. Similarly, the roll-strip contact is dynamic and the shape and size of micro-contacts may vary throughout the roll bite. Nevertheless, it is reasonable to assume, on average, that the number of micro-contacts and their size distribution remain constant for a given rolling condition.

In the next step, the volume of material removed as wear debris at each micro contact is determined. To attain this objective, each contacting asperity is approximated by an elliptical-paraboloid. The size and shape of the elliptical-paraboloid is determined using the least squares fit through the measured height data of the contacting asperity. Next, the degree of penetration of each micro-contact is computed. The

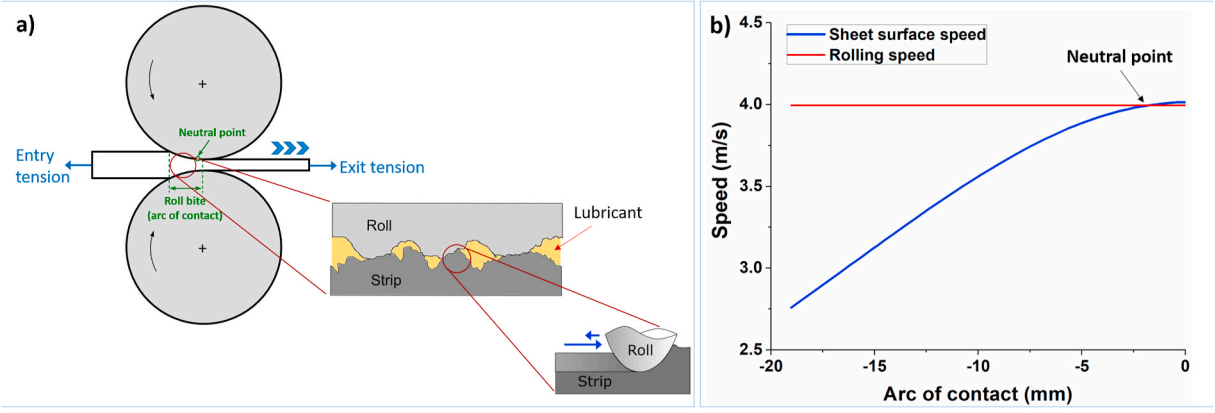

Fig. 1. a) schematic of the multiscale contact geometries during cold rolling, and b) an example of the speed differences between the sheet (blue) and roll surface (red) throughout the roll bite as a function of the arc of contact (0 = exit). (For interpretation of the references to color in this figure legend, the reader is referred to the Web version of this article.)

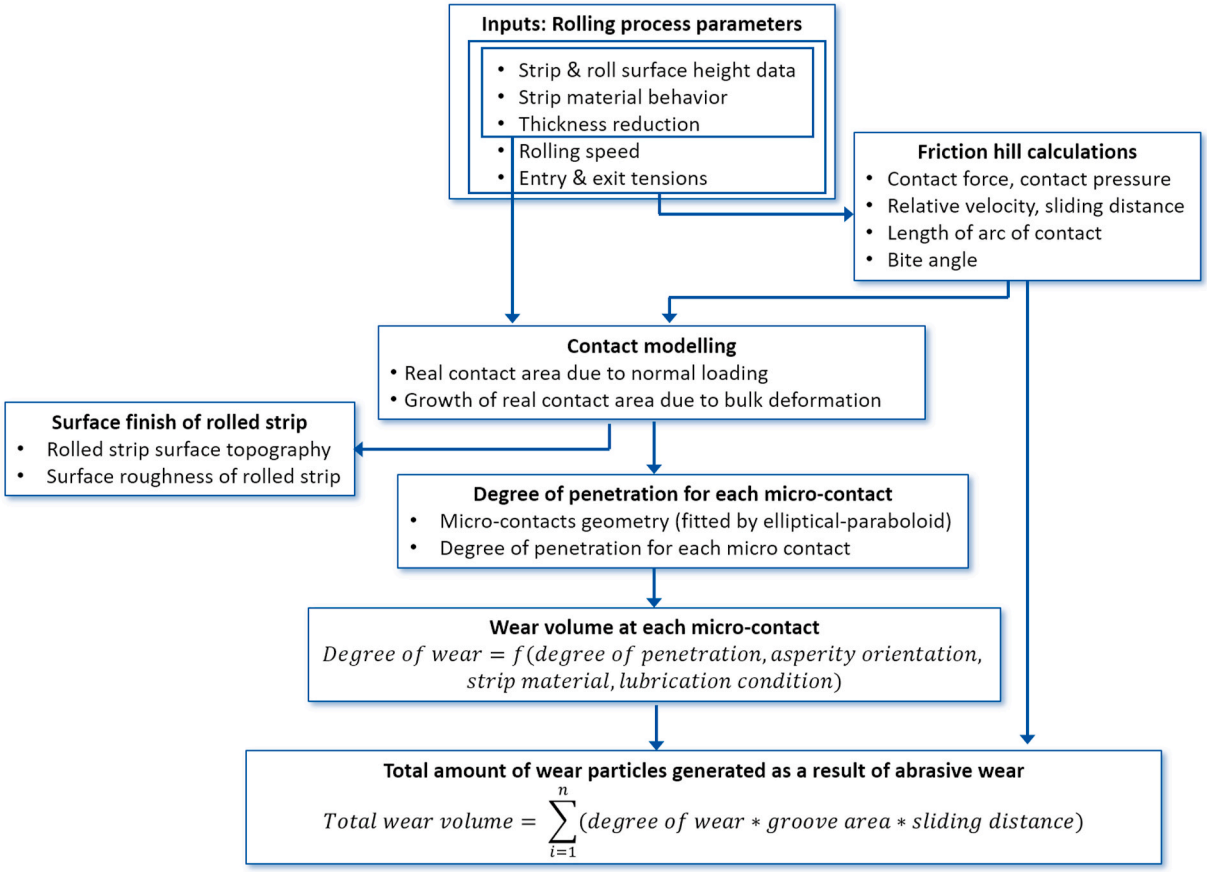

Fig. 2. Flow diagram of the computational approach used to model wear in cold rolling.

degree of penetration (d_p), which is the ratio of indentation depth (d) and the semi-axis of the contact spot in sliding direction (a) is a commonly used non-dimensional measure of the sharpness of an indenting asperity [16,17]. For a spherical indenter, d_p is defined by (also see Fig. 3a):

$$d_p = d/a \tag{1}$$

The degree of penetration calculation of the elliptic paraboloid asperities is made by adjusting the value of degree of penetration of a sphere by introducing the shape and the orientation (θ) of the asperity with respect to the sliding direction as described in Ref. [17]. The semi-axis of the contact in the sliding distance is expressed in terms of the orientation of the asperity and the semi-minor and semi-major axis of the contact (see Fig. 3b) as:

$$a_x' = \sqrt{\left(a_x^2.a_y^2\right) \Big/ \left(a_x^2.\sin^2\theta + a_y^2.\cos^2\theta\right)} \tag{2}$$

with this, Eq. (1) becomes:

$$d_p = d \Big/ a_x' = d \Big/ \sqrt{\left(a_x^2.a_y^2 \Big/ \left(a_x^2.\sin^2\theta + a_y^2.\cos^2\theta\right)\right)} \tag{3}$$

Next, the proportion of material removed as wear debris, denoted by the degree of wear (d_w), at each micro contact is evaluated. The degree

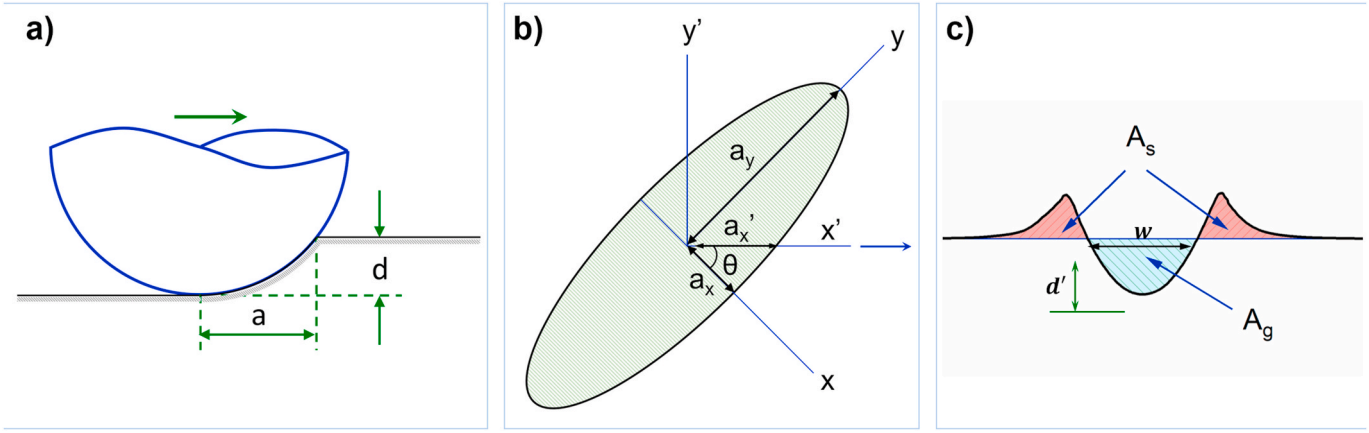

Fig. 3. a) degree of penetration for a spherical indenter, b) an elliptic micro-contact: x' is the sliding direction, a_x and a_y are the semi-minor and semi-major axis, respectively, and c) cross section of a scratch wear scar.

of wear for a given contact geometry and normal load depends on material properties and surface treatment of the interacting surfaces, surface chemistry, contact temperature and lubricant composition. Because d_w depends on many variables, the values are obtained in this work by performing scratch experiments using an indenter made from a tool steel, having a similar composition as commonly used work roll material, sliding against a polished strip material surface. The details of the scratch experiments are discussed in section 3.2. d_w can be calculated from the average two-dimensional scratch cross section (illustrated in Fig. 3c) by:

$$d_w = (A_g - A_s)/A_g \tag{4}$$

The volume of material removed due to wear at each micro contact is the product of the degree of wear, frontal area of the groove (A_g), and the sliding distance (L). The sliding distance is determined in the friction hill calculations from the relative sliding speed of the roll and the strip surface in the roll bite. The frontal area of the groove A_g can be approximated by eq. (5) [18], see also Fig. 3c:

$$A_g = \frac{2}{3}.w.d' + d'^3 \Big/ (2.w) \tag{5}$$

Finally, the total volumetric wear (V) caused by all asperities is calculated as the sum of the volume of material removed due to abrasive wear at each micro contact:

$$V = \sum_{i=1}^{N} (L.d_w.A_g) \tag{6}$$

where, N is the number of micro-contacts.

3. Materials and experiments

3.1. Rolling experiments

The objective of the rolling experiments was to validate the proposed wear model and to investigate the effect of rolling parameters such as roll roughness, thickness reduction, lubrication, entry/exit stresses and rolling speed on strip cleanliness. The rolling experiments were carried out on a two-high configuration, semi industrial rolling mill in Tata Steel, The Netherlands. An illustration of the rolling mill configuration is presented in Fig. 4. Two sets of work rolls with r.m.s. roughness (Sq) of 0.1 μm ('smooth' rolls) and 1.2 μm ('rough' rolls) were prepared to study the effect of roll roughness on wear particles generation. The roughness peaks of a freshly ground roll wear off quickly in the beginning of its service life. To avoid this undesired roughness change, dummy rolling experiments were conducted before the main experiments. The diameter of the rolls is 400 mm. The strip material was an industrially hot-rolled and pickled Titanium-stabilized interstitial-free (Ti-IF) steel, a steel grade widely used in automotive outer body part applications. The entry strip was 3 mm thick and 100 mm wide. A fully formulated industrial rolling (mineral) oil that contains anti wear and extreme pressure additives was used in the rolling experiments. Pure oil was used instead of an emulsion to avoid the influence of undesired oil concentration variation and emulsion contamination during circulation. However, note that using an emulsion is a common practice in industrial production. The lubricant was applied on the strip before entering the roll bite using a direct application unit (Fig. 4). The oil temperature was maintained between 43 °C – 45 °C. There was no oil circulation. The rolling force, torque, thickness, rolling speed, entry and exit strip speeds, and entry and exit tension forces were measured during the experiments.

The effect of thickness reduction was examined by performing rolling experiments at 5%, 10%, 20% and 35% thickness reduction. The rolling speed was varied between 0.5 and 2.0 m/s. The experiments were carried out both in lubricated and dry (non-lubricated) conditions. The effect of forward slip was studied by varying the exit tension between 10 and 40 kN (83–167 MPa) while keeping the entry tension constant at 20 kN (67 MPa). Varying the entry and exit tension affects the location of the neutral point, and thereby, the forward slip [15]. Forward slip (S_{fwd}) is defined as the relative difference between the peripheral roll speed (V_r) and strip exit speed (V_{exit}), and is given by:

$$S_{fwd} = (V_{exit} - V_r)/V_r \tag{7}$$

Prior to the rolling experiments, the coils were degreased and cleaned using a commercial cleaner (3% concentration) to remove oil residues from previous processes, using a direct application unit. The cleaner was applied using a flat jet nozzle at the entry side of the mill. The cleaner is then blown off with an air knife while moving at a speed of 0.2 m/s on the exit side of the mill. A summary of the process parameters of the rolling experiments are presented in Table 1. A total of 400 m of strip was rolled, 10 m for each rolling experiment.

The 3D surface roughness of the strip before and after rolling as well

Table 1
Process parameters of the rolling experiments.

Experiment No.	Roll roughness, Sq (μm)	Lubrication condition	Thickness reduction (%)	Rolling speed (m/s)	Exit tension (kN)
1–4	0.1	Dry	5, 10, 20, 35	0.5	10
5–7			20	0.5	20, 30, 40
8–10			20	1.0, 1.5, 2.0	10
11–14		Lubricated	5, 10, 20, 35	0.5	10
15–17			20	0.5	20, 30, 40
18–20			20	1.0, 1.5, 2.0	10
21–24	1.2	Dry	5, 10, 20, 35	0.5	10
25–27			20	0.5	20, 30, 40
28–30			20	1.0, 1.5, 2.0	10
31–34		Lubricated	5, 10, 20, 35	0.5	10
35–37			20	0.5	20, 30, 40
38–40			20	1.0, 1.5, 2.0	10

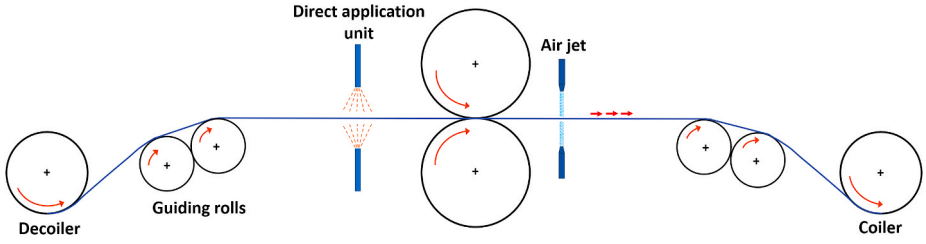

Fig. 4. Schematics of the pilot-mill used for the rolling experiments.

as the rolls was measured using a Sensofar S-neox confocal microscope. The surface roughness of the rolls was measured by replicating the roll surface using a surface replicating compound. Form removal was performed on the roughness measurements to remove tilt and eliminate the long-range wavelengths associated with lack of flatness.

The surface cleanliness of the rolled strip was evaluated using two widely used methods in the steel industry. The first one is the "reflection tape" method. In this method, an adhesive tape is applied on the surface of the rolled strip (with a thumb). The tape is then removed and it is taped on a white paper. Afterwards, a light source is directed to the tape on the paper and the reflected light is measured. The fraction of the reflected light is a measure for the degree of cleanliness of the strip. The reflection is 100% for an entirely transparent tape and 0% for an entirely black one. The better the surface cleanliness of the strip, the higher the reflection value. Typical reflection values for steel rolling are between 40% and 80% [3]. The second method, known as "iron tape method", involves measuring the weight of (iron) wear particles per unit area. Wear particles in steel cold rolling consist mostly of iron [2]. The wear debris are removed from the rolled strip surface using an ash-less adhesive tape. The tape is burnt afterwards and the weight of the remaining wear debris is measured.

Both the reflection tape and iron tape method do not provide information about the size and shape of wear particles. Hence, analysis of the quantity and size distribution of the wear particles was performed using image processing. This was done first by taking a color microscopy image of the wear particles collected on a transparent adhesive tape, which is placed over a black sample holder to facilitate particle identification and extraction, at high magnification. The images are then converted into a gray scale image. The wear particles are extracted from the image based on contrast information by removing the background. Next, the area and size of each particle is measured. Finally, particle size distribution analysis is carried out.

3.2. Scratch experiments

Scratch experiments were performed to evaluate the volume of material removed as wear debris at each micro contact when a roll asperity ploughs through the strip surface. The scratch experiments were designed to resemble the roll asperity-strip contact in the roll bite of cold rolling processes. The experiments were executed using a Multi-purpose tribometer (Bruker's UMT Tribolab). The experiments were conducted using conical indenters with a hemispherical tip under lubricated conditions, which represents the roll asperity, sliding against a polished flat strip substrate, as depicted in Fig. 5. The hemispherical tip has a radius in the order of a single roughness asperity of the roll (175 μm). The strip samples were polished to a mirror like surface finish with an average r.m.s. roughness of less than 20 nm. The scratch indenters were made of a hardened and tempered medium cold working tool steel (60–62 HRC) that has similar composition to a commonly used work roll material. The substrate was a piece of strip obtained from the hot rolled and pickled Ti-IF steel coil used in the rolling experiments. The same oil-type used in the rolling experiments was used in the scratch experiments.

The strip sample and the indenters were degreased and cleaned using acetone and isopropanol prior to the scratch experiments. Next, an oil film was applied on the strip sample. Each scratch was made by applying the desired normal load under load-controlled conditions. The load needed to obtain the intended d_p was determined on the basis of the radius of the indenter tip and hardness of the strip material. The scratches were performed using a constant normal load, ranging between 3 and 39 N. The sliding speed was kept constant at 1 mm/s. The length of each scratch is 15 mm. The normal force, the tangential force and the friction coefficient were measured during the experiments.

The three-dimensional height profile of the scratches was measured using confocal microscopy (S neox 3D Optical Profiler from Sensofar). Tilt correction and shifting the reference plane to $z = 0$ was carried out employing the flat section away from the wear track which is unaffected by the scratches. The amount of material removed as wear debris, for each individual scratch, was measured from the wear groove profile by calculating the degree of wear (d_w) from the ratio of the groove volume and shoulder volume, see Eq. (4).

4. Results & discussion

4.1. Rolling experimental results

4.1.1. Roughness changes

The surface roughness topographies of the rolled strip are presented in Fig. 6 and Fig. 7. The r.m.s. roughness (Sq) of the strip after cold rolling is plotted in Fig. 8. The following points can be noted from these figures: (i) thickness reduction is the predominant rolling parameter that determines the real contact area, and hence, the roughness of the rolled strip (Figs. 6 and 8); (ii) rolling speed and exit tension had little impact on the rolled strip roughness for a given thickness reduction, both in the lubricated and dry experiments (Figs. 7 and 8); (iii) the real area of contact is much higher in the case of dry rolling experiments than the lubricated ones for a given thickness reduction, see Figs. 6–8. These observations are preliminary indicators of which rolling parameters may potentially have major influence on wear particles formation (strip cleanliness).

The roll marks become predominant and the strip asperity flattening

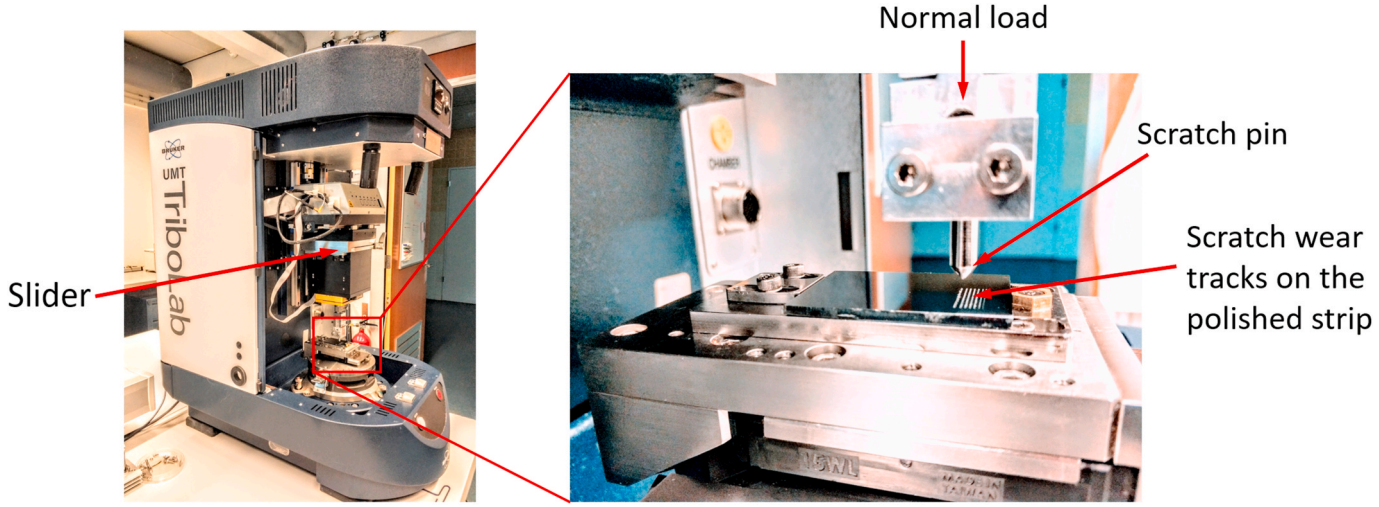

Fig. 5. Scratch experiment setup.

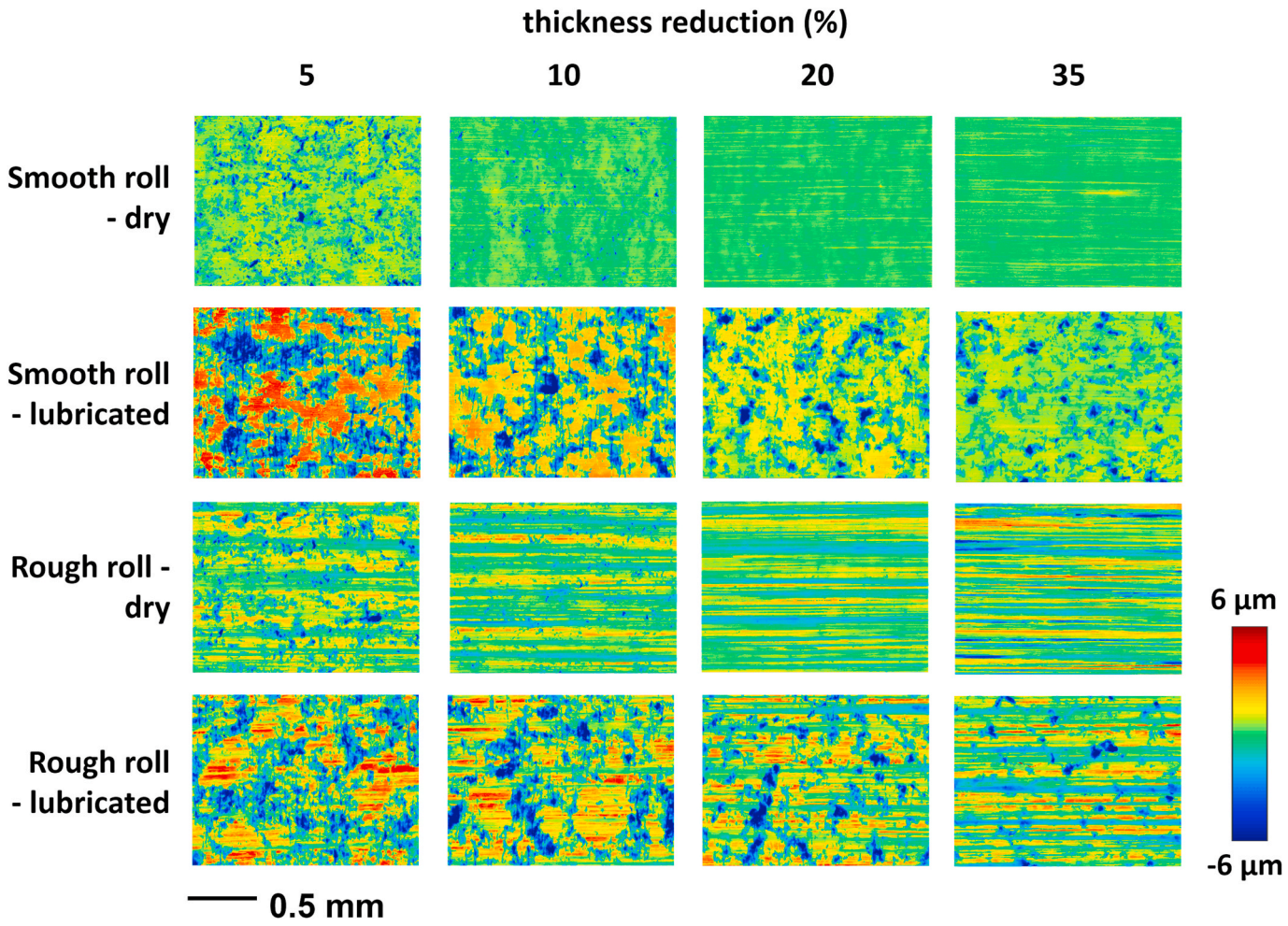

Fig. 6. Roughness topography of the rolled strip as a function of thickness reduction in dry and lubricated conditions, using smooth and rough rolls.

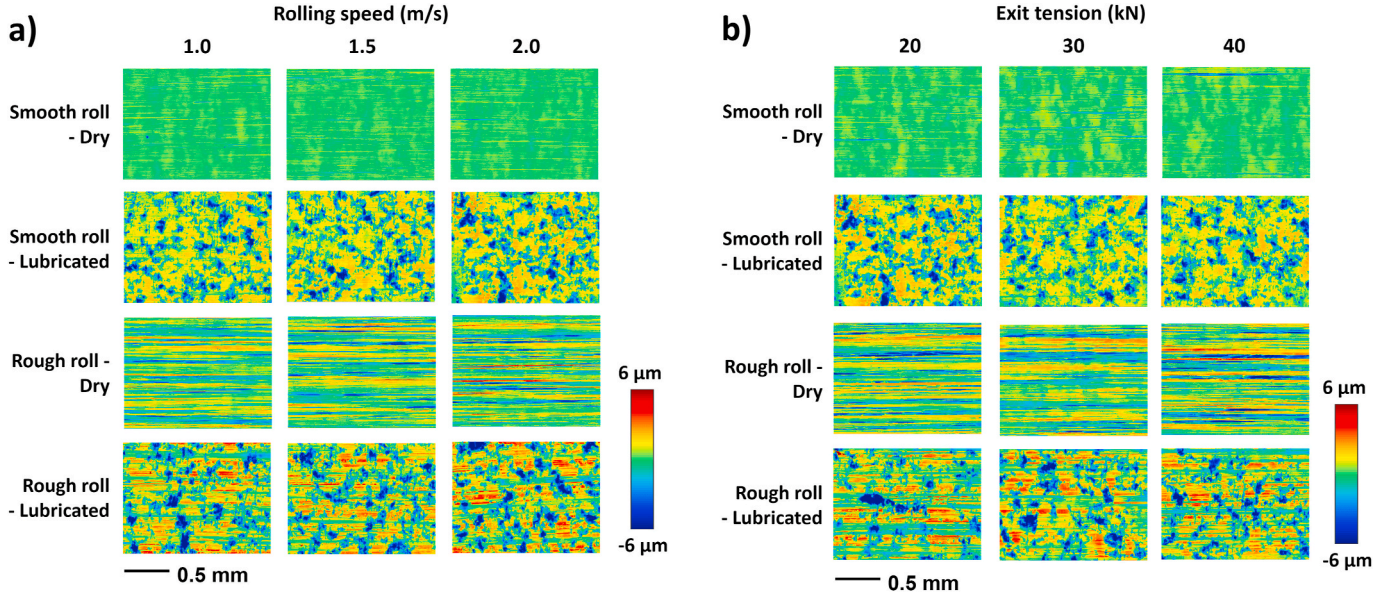

Fig. 7. Roughness topography of the rolled strip as a function of: a) rolling speed (at 20% thickness reduction and 10 kN exit tension) and b) exit tension (at 20% thickness reduction and 0.5 m/s rolling speed).

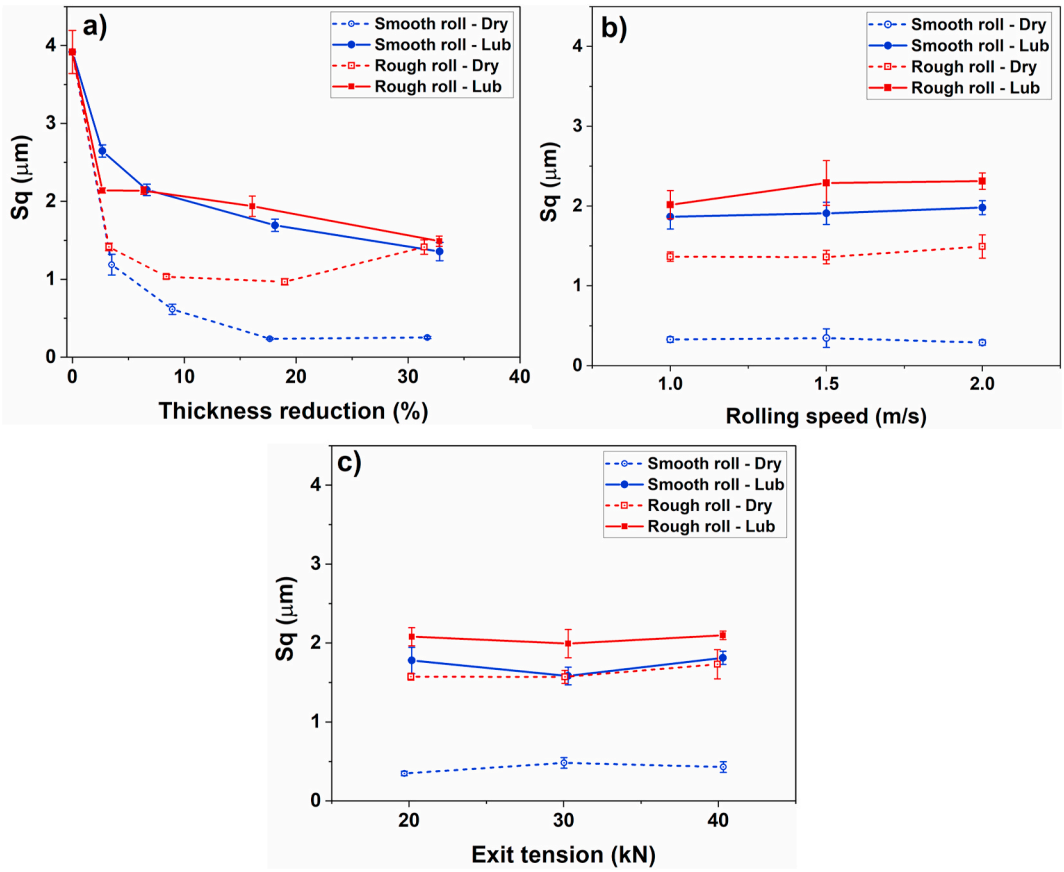

Fig. 8. R.m.s. surface roughness of the rolled strip as a function of: a) thickness reduction, b) rolling speed, and c) exit tension.

and/or indentation intensify with an increase in the thickness reduction. This translates to a higher real contact area ratio (i.e. the ratio of the real contact area to the apparent contact area) and more conformity of the strip to the roll surface with an increase in thickness reduction. It is known that bulk deformation dramatically increases asperity flattening and indentation [14,19]. The roughness topography of the incoming strip is completely obliterated at 20% thickness reduction in the dry rolling experiments, indicating full contact between the strip and the roll. On the other hand, roughness features of the strip from the pickling process, particularly the cavities, are still clearly visible in the lubricated rolling experiments at 35% thickness reduction. This is even more pertinent on the strip rolled using smooth rolls. Rolling speed is expected to have no or little impact on the real area of contact for a rolling process that operates under the boundary lubrication regime, as there are basically no velocity dependent effects. The little impact of the rolling speed on the rolled strip roughness confirms that the current lubricated rolling experiments were indeed operating mainly under boundary lubrication conditions. Similarly, the variation of the exit tension did not affect the roughness of the rolled strip. This is expected as the thickness reduction was kept constant.

One factor that plays an important role in the real contact area ratio difference between the dry and the lubricated experiments is the lubricant trapped in the cavities [20,21]. Huart et al. [7], using two dimensional FEM simulations, demonstrated that a trapped lubricant avoids the total flattening of asperities and limits the real contact area ratio. With the roll-strip relative motion, lubricant may be trapped in a closed volume at the entry of the roll bite, particularly for smooth rolls. It is squeezed and dragged into the roll-strip interface resulting in the so called micro-plastohydrodynamic lubrication (MPHL) [21–24]. MPHL is the trapping of lubricant in closed surface cavities and the subsequent permeation of the trapped lubricant into the neighboring real contact area due to deformation. This lubricant film prevents direct metal to metal contact and allows the conservation of the cavity geometry. Due to the strong directionality on the roughness, lubricant trapping can be expected to be negligible in the rolling experiments when rough rolls are used, as the squeezed lubricant can escape through the grooves created by the roll roughness [25]. This is clearly visible at the highest thickness reduction, where a relatively low number of cavities are seen on the strip surface rolled using rough rolls (Fig. 6). Another contributing factor that explains the difference in the real contact area ratio between the dry and the lubricated experiments is junction growth. Tabor [26] has demonstrated that the real area of contact increases as the tangential force is increased. Junction growth continues until the tangential shear stress reaches the interface shear strength, where macroscopic sliding onsets. Obviously, a higher tangential force is needed for macroscopic sliding to occur in the dry rolling experiments than the lubricated ones. Hence, the real contact area is higher in the dry rolling experiments.

Another characteristic of the dry rolling experiments is the material pickup that occurred for the rolling experiments with rough rolls at 35% thickness reduction. This is evidenced by the “scratches” that started to appear on the rolled strip surface topography at 35% thickness reduction (Fig. 6) and the increase of the Sq value (Fig. 8a). Once full contact is reached, which is already achieved at 20% thickness reduction, the Sq is expected to stay constant. However, the Sq increased at 35% thickness reduction. This can only be attributed to the increase of the roll roughness due to material pickup. This roughness change is also reflected in the subsequent experiments, see Fig. 7. Deep scratches, although few, that indicate material pickup by the roll are also seen on the strips rolled using smooth rolls (Fig. 7). This observation may be explained by the fact that rough rolls provide much more surface irregularities and surface defects that serve as an initiation point for material transfer (galling) than the smooth rolls [27]. This indicates that

a combination of rough roll and high thickness reduction are not favorable in terms of strip cleanliness as this may lead to galling and more wear.

4.1.2. The effect of rolling parameters on wear particles formation

4.1.2.1. Thickness reduction, roll roughness and lubrication. The plots of iron tape and reflection tape values, indicating surface cleanliness of the sheet material after the rolling experiments, as a function of thickness reduction are provided in Fig. 9. The amount of material removed as wear particles increases with the thickness reduction; higher thickness reduction leading to higher wear and dirtier strip. Higher thickness reduction means harsher contact conditions, i.e. higher rolling forces (Fig. 10a) and higher contact stresses (Fig. 10b), higher real area of contact, increased length of the arc of contact, higher sliding lengths, higher interfacial temperature, and higher depth of indentation by roll asperities. In addition, high thickness reduction increases the roll bite angle which may reduce the amount of trapped lubricant [7]. These contact conditions promote higher rate of wear particles formation. Furthermore, higher thickness reduction may result in more material pickup as it increases the sliding length, normal stress and contact time which promote adhesion and adhesive wear [11]. This was manifested in the roughness profiles of the rolled trip, particularly for the dry rolling experiments, as discussed earlier in section 4.1.1.

The impact of thickness reduction on strip cleanliness is far greater for the rolling experiments using rough rolls than for smooth rolls. When the thickness reduction was increased from 5% to 35% in the lubricated experiments, the amount of wear particles (mg/m^2) increased by approximately 9 times for the rough rolls while it increased only 3 times for the smooth rolls, see Fig. 9a. Likewise, the amount of wear increased by 7.5 times for the rough rolls and by only 2.5 times for smooth rolls in the dry experiments. The amount of wear at 35% thickness reduction in the case of rough rolls is 15 times higher than in the case of smooth rolls in the lubricated experiments, while it is only 2.4 times in the dry ones. These results clearly demonstrate that roll roughness has a major influence on wear particles formation and strip cleanliness in particular. The smoother the work roll, the better is the strip cleanliness. The asperities of rough rolls plough deeper into the strip material, increase the frictional stress [28] and result in more wear. These results corroborate with earlier studies [3,5] which demonstrated that strip cleanliness strongly deteriorates when the roll roughness is increased. The proportion of asperities operating in the cutting and wedge forming abrasive wear regimes (i.e., the wear regimes which lead to wear particles generation) increases with the increase in the roughness of the rolls. This is related to an increase in the average degree of penetration (d_p) of the roughness asperities as the roughness of the rolls increases. A schematic representation of the different abrasive wear modes as a function of d_p and interfacial shear strength ratio f (i.e. ratio of interface shear strength over shear strength of the softer material) is depicted in Fig. 11.

Although it is sometimes possible to roll without lubrication, in general lubricant is applied during cold rolling (in the form of an emulsion) to act as a coolant, to prevent surface damage and to control friction. Nevertheless, the deformation of surfaces under unlubricated conditions provides a useful starting point for lubricated rolling, and points up the key features in the mechanics of asperity deformation. The influence of lubrication on strip cleanliness is also clearly seen in Fig. 9. The strips rolled under lubricated conditions have a lower surface cleanliness than those in dry conditions at a given thickness reduction for the rolling experiments using rough rolls. On the contrary, the strips rolled using smooth rolls in lubricated experiments are cleaner than the dry ones. This can be explained by the differences in the active abrasive wear modes in dry and lubricated conditions, the effect of lubrication on the real contact area, and the average degree of penetration of the roughness asperities of the rough and smooth rolls. The main cause of this difference is the difference in the interfacial shear strength between the dry and the lubricated contact, which affects the local contact pressure and friction stress on each asperity.

Under dry rolling the friction is high, and therefore f is high, and as a result mainly wedging and cutting takes place, see Fig. 11 [16]. Lubrication reduces the shear strength at the contact interface. The reduced interfacial shear strength results in the transition of the wear mode from wedge forming to cutting for the asperities with d_p higher than the critical degree of penetration corresponding to the transition from ploughing to wedge forming/cutting (d_{p_pwc}). For asperities with $d_p < d_{p\_pwc}$, lubrication has little influence on the wear mechanism and they stay in the ploughing wear mode [29]. Thus, the roll asperities operate primarily either in ploughing or cutting regime in the lubricated rolling experiments. A higher proportion of the wear groove volume is removed as wear particles in the cutting wear mode than in wedge forming [16,29,30]. Owing to the higher average d_p of the rough roll asperities than the smooth ones, more asperities will transition from wedging to cutting in the former as a result of the lubrication. This explains the higher wear of the lubricated experiments compared to the dry ones when using rough rolls. In contrast, a small proportion of asperities are expected to have a d_p greater than d_{p_pwc} in the smooth rolls, hence little increase in wear particles is expected as a result of the lubrication. The decrease of the wear particles in the lubricated experiments compared to the dry ones when rolling using smooth rolls can be explained by the reduction in the real area of contact due to lubricant entrapment, see section 4.1.1. More lubricant trapping is expected when smooth rolls are used compared to the rough rolls, as the lubricant can easily escape on the deep ridges created by the rough roll asperities. Moreover, the lubrication regime of the smooth rolls will be more towards the mixed lubrication regime, resulting in less real contact area

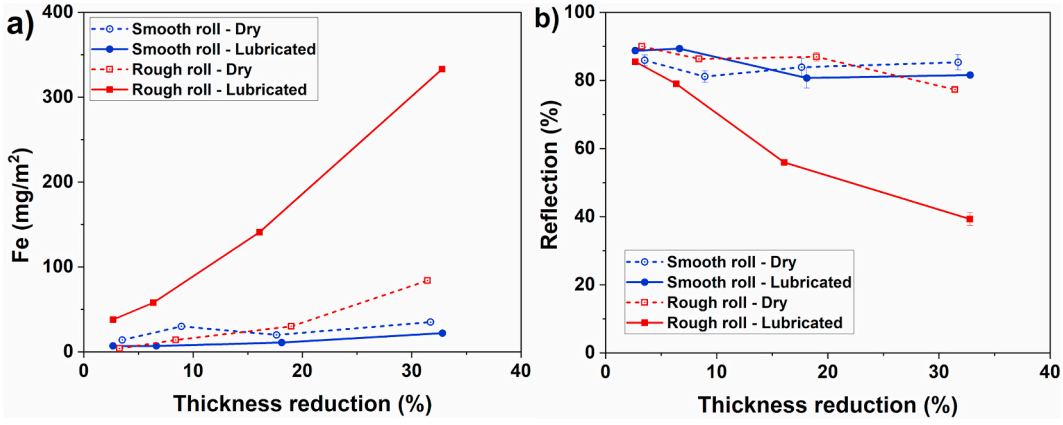

Fig. 9. Iron tape a) and reflection tape b) values as a function of thickness reduction.

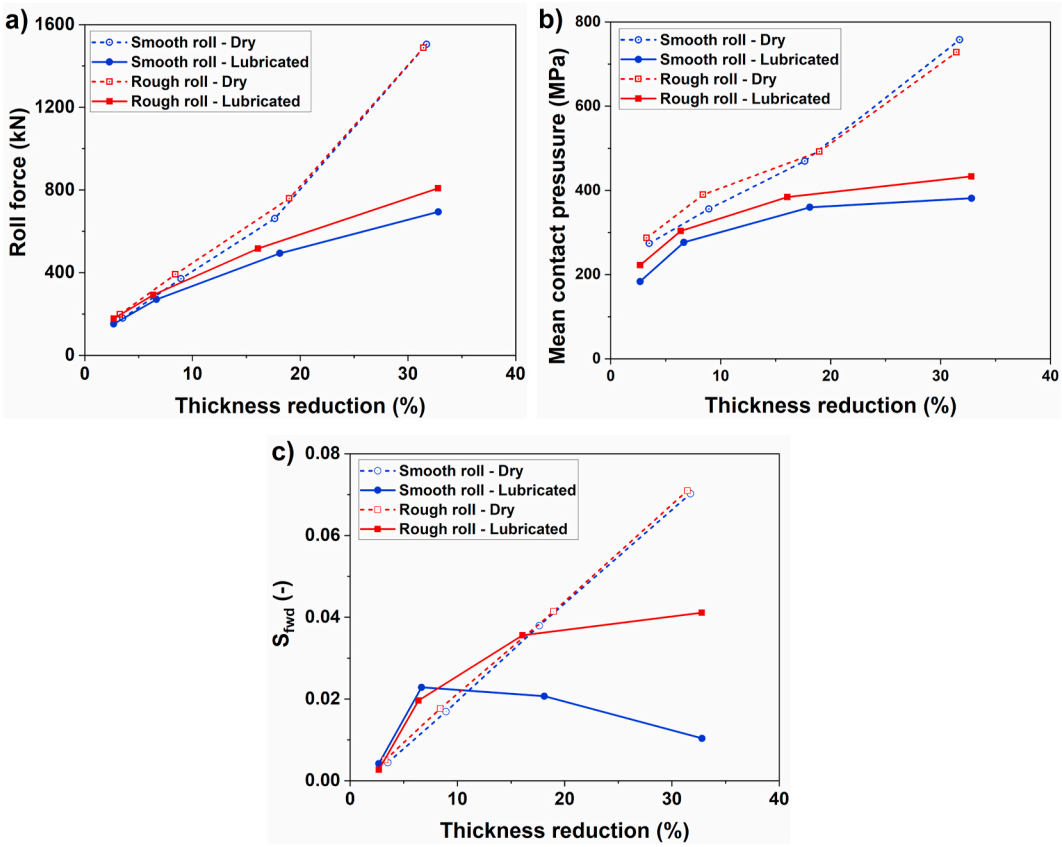

Fig. 10. Relation between: (a) thickness reduction and rolling force, (b) thickness reduction and mean contact pressure and (c) thickness reduction and forward slip.

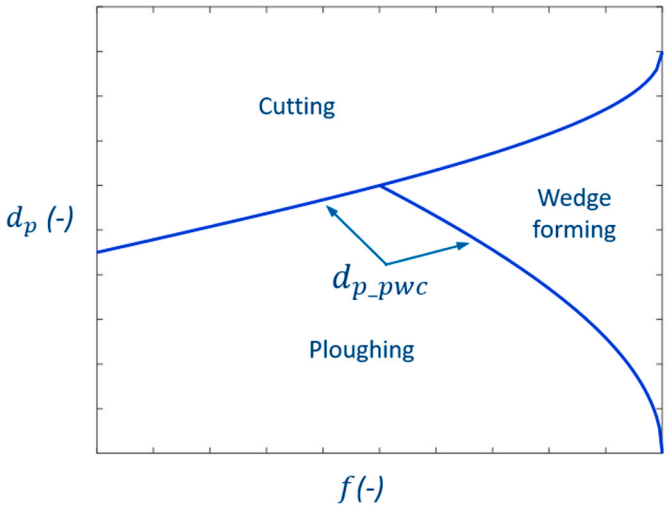

Fig. 11. Schematic representation of abrasive wear mode diagram, after Hokkirigawa and Kato [16,29].

between the roll and the strip, and hence, less friction and wear. This is attested by the lower rolling force (Fig. 10a) and lower forward slip (Fig. 10c) of the rolling experiments using smooth rolls. Low forward slip is commonly associated with low friction coefficient [31].

4.1.2.2. Rolling speed. Reflection tape and iron tape values as a function of the rolling speed are plotted in Fig. 12. The thickness reduction was kept constant at 20%. Rolling speed did not show any substantial influence on the strip cleanliness. In literature [3], a positive influence of a high rolling speed on surface cleanliness is reported. This influence can be expected for a very large increase in the rolling speed for lubricated cold rolling. As this may result in thicker oil film in the roll bite and affect the lubrication regime (possibly change from boundary lubrication to mixed lubrication) and therefore reduce the real contact area. The fact that the rolling speed did not significantly affect the strip cleanliness in the current experiments affirms that the rolling was indeed carried out in boundary lubrication regime and the variation of the rolling speed was not big enough to considerably influence the film thickness and the lubrication regime. Both the rolling force and forward slip were not influenced notably by the rolling speed (Fig. 13), corroborating the strip cleanliness measurements. The small increase in the rolling force as the rolling speed is increased (Fig. 13a) is probably caused by the strain rate hardening behavior of the strip material. The slight decrease of the forward slip observed in Fig. 13b, particularly for the lubricated rolling experiments with smooth rolls, indicates that there might be a marginal increase in film thickness.

4.1.2.3. Exit tension. The exit tension was varied, keeping the entry tension constant, to investigate the influence of forward slip on strip cleanliness. Increasing the exit tension moves the neutral point towards the roll entrance and increases the forward slip [15]. One effect of varying the forward slip is on the sliding length before and after the neutral point. The strip asperities are deformed by the ploughing roll asperities in the rolling direction before the neutral point. Strip asperities are deformed opposite to the rolling direction after the neutral point, as the relative velocity of the roll asperities relative to the sheet surface is reversed. The effect of changing the exit tension on forward slip is illustrated in Fig. 14. The rolling speed and thickness reduction were kept constant at 0.5 m/s and 20% respectively. As expected, the forward slip increased with an increase in the exit tension. Besides, the increase in forward slip is much higher for the lubricated rolling experiments than the dry ones. This can be ascribed to the lower friction

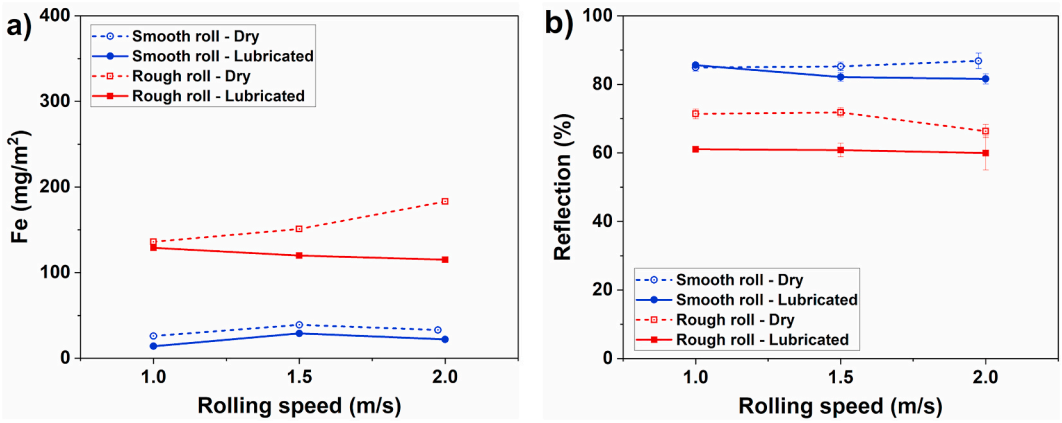

Fig. 12. Iron tape a) and reflection tape b) values as a function of the rolling speed.

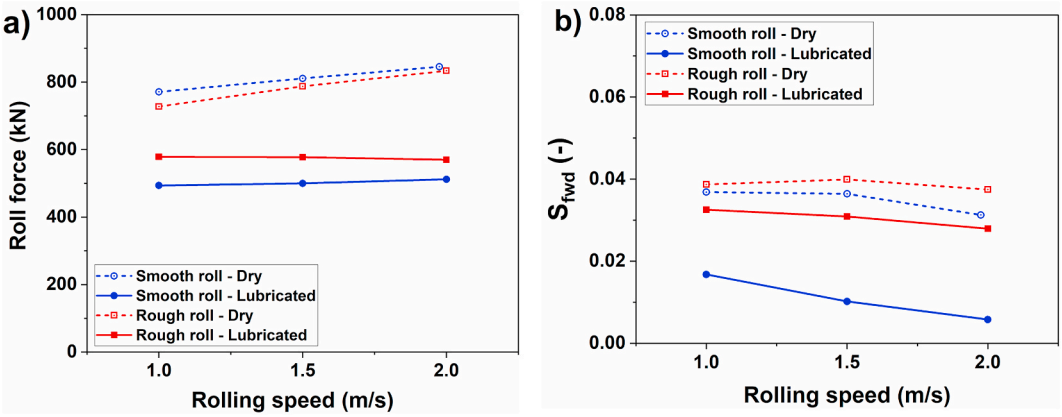

Fig. 13. Influence of rolling speed on: a) rolling force and b) forward slip.

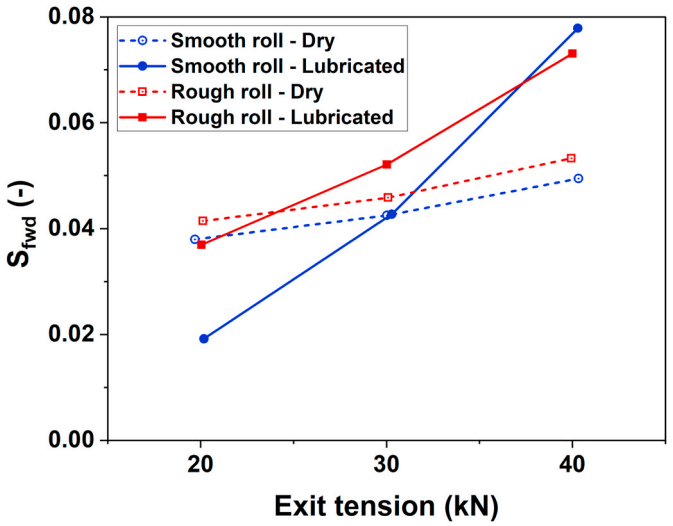

Fig. 14. Influence of exit tension on forward slip.

coefficient of the lubricated experiments which allows easy slip between the roll and the strip surface.

The amount of wear debris produced as a function of the forward slip is plotted in Fig. 15. No clear influence of the forward slip on the rate of wear particles formation is witnessed in the current experiments. Contradicting results are reported in literature on the influence of forward slip on strip cleanliness. Some studies [6,7] reported increasing the forward slip increases the amount of wear particles generated. Others [3, 8] reported no influence of forward slip on the quantity of wear particles. The current result agrees with the latter. Deltombe et al. [6] and Huart et al. [7] claimed that increasing the forward slip contributes to the increase in quantity of wear particles produced, with its influence being more pronounced at high thickness reductions and high forward slip. This was attributed to the large sliding distance in the backward direction. However, the forward slip in their study is much higher (>0.1 and >0.2) than the one experienced in the current experiments (<0.08).

4.1.2.4. Reflection tape vs iron tape. In order to study the reproducibility and suitability of the two strip cleanliness characterization techniques, the relationship between the reflection tape and iron tape measurement values is plotted in Fig. 16. They seem to show an exponential relationship. The exponential relationship can be linked to the fact that overlapping wear particles cannot be measured in reflection tape measurements, whereas all the particles are measured in the iron tape measurements. One effect of this relationship is that the reflection tape is less sensitive for unclean strips. Note that the lubricated and the dry experiments do not lie on the same curve. The reflection tapes of the lubricated experiments are darker than the dry ones for the same amount of iron tape value. This is expected as the lubricant makes the tape darker in the lubricated experiments. Jacobs et al. [3] has evaluated the accuracy of the reflection tape and iron tape method. They showed a linear relationship between these two methods in a semi-logarithmic scale.

4.1.3. Wear particle size distribution

Analysis of the size distribution of wear particles has been done using

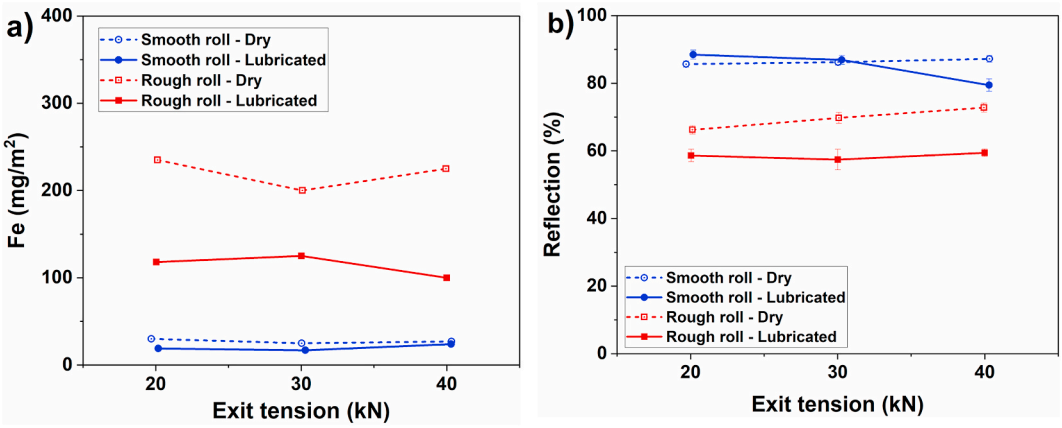

Fig. 15. Strip cleanliness as a function of exit tension.

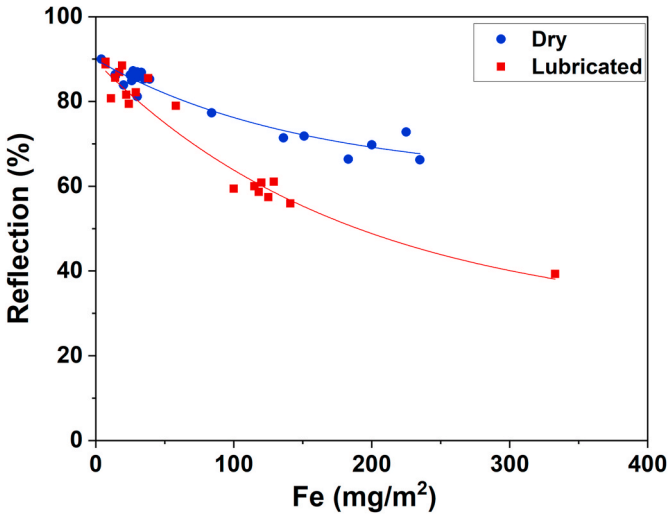

Fig. 16. Reflection tape vs iron tape values.

microscopy imaging and image segmentation. This allows to visualize the shape and/or size of the wear particles, and to study how the characteristics of the particles change (if any) with process parameters. The typical acquired color images are presented in Fig. 17a. The wear particles are clearly brighter than the background. After converting the color image into gray scale, the wear particles are extracted from the image based on contrast information by thresholding to remove the background. It is necessary to know the distribution of the pixel values to obtain an appropriate threshold. The histogram of the image in Fig. 17a is shown in Fig. 18. The distribution of the background is concentrated around and below the highest peak of the histogram distribution. The distribution of the pixel values in all the images taken show a peak approximately in the same range as in Fig. 18 because the background luminescence is adjusted during image acquisition. Consequently, the pixels corresponding to the wear particles can be distinguished from those belonging to the background by the following condition:

$$Pixel\ value > \zeta \tag{8}$$

where, ζ is the appropriate threshold.

The wear particles can be extracted by selecting the pixels which

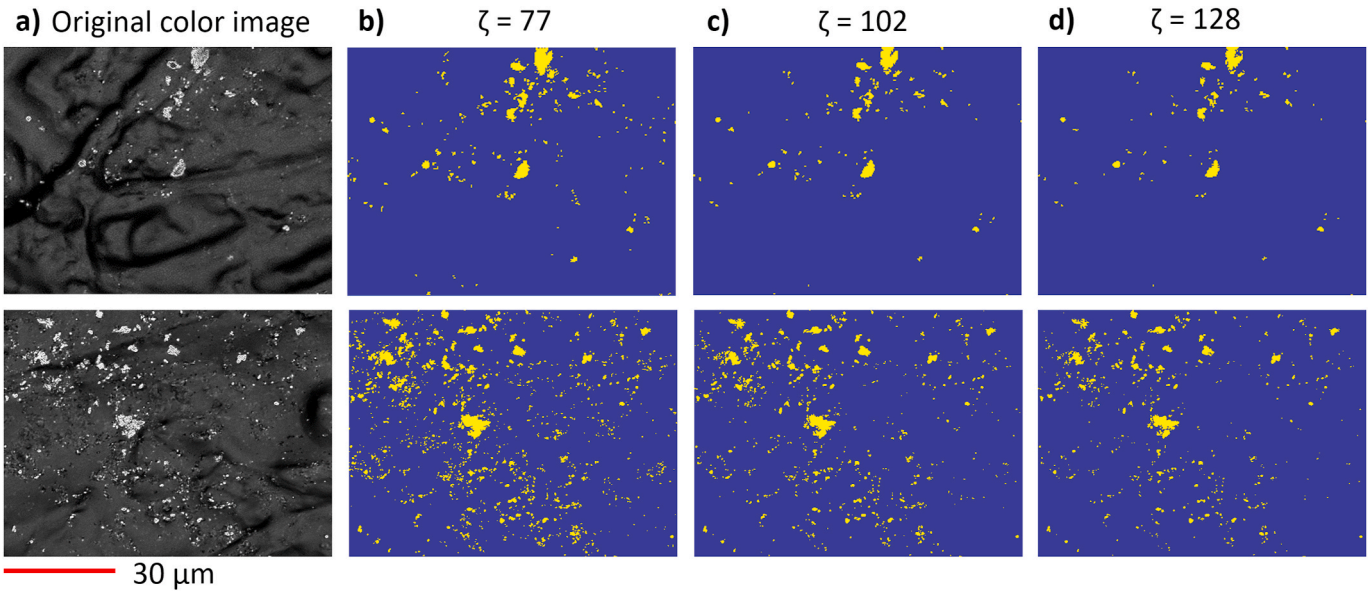

Fig. 17. a) typical color microscopy images of the wear particles of the rolling experiments, and b-d) the corresponding images after wear particle extraction (represented by light yellow) by applying several threshold (ζ) values. (For interpretation of the references to color in this figure legend, the reader is referred to the Web version of this article.)

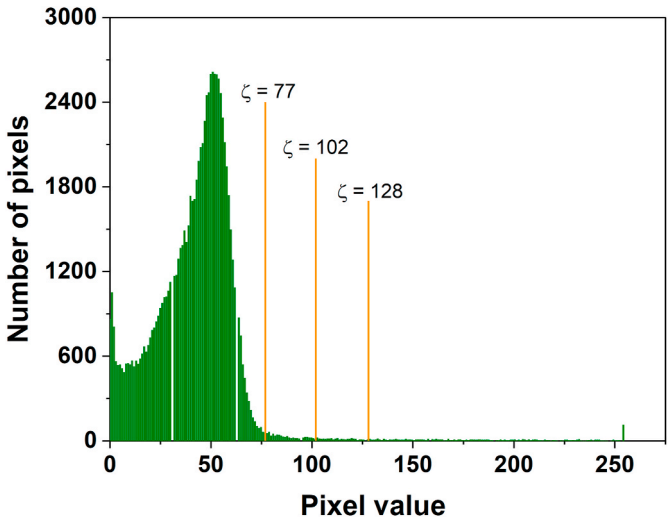

Fig. 18. Histogram of pixel values of the image in Fig. 17a (top).

satisfy the conditional expression in Eq. (8). Fig. 17b-d shows the result when the wear particles are extracted from the images in Fig. 17a for several ζ values. A closer look of the images shows that part of the background is falsely identified as a wear particle at $\zeta = 77$ (30% of the maximum pixel value) (Fig. 17b) and some wear particles (mainly contaminated small wear particles) are falsely identified as background at $\zeta = 128$ (50% of the maximum pixel value). A threshold value of $\zeta = 102$ (which is 40% of the maximum pixel value) was chosen for further analysis as this value appears to minimize false interpretation of the background as a wear particle and vice versa. After the particles are identified from the input image, the size (area and equivalent diameter) of each particle and the number of particles on each image is determined. The image processing was executed in MATLAB.

Fig. 19 illustrates the spread of wear particles on the adhesive tape at several thickness reductions, roll roughness and lubrication condition. A lot of small and a few big wear particles are seen dispersed throughout the tape. Previous study [2] has shown that these particles consist mostly of iron. The size and quantity of wear particles increase as the thickness reduction increases. This is consistent with the iron tape and reflection tape measurements. The increase in the size of wear particles as the thickness reduction is increased can be ascribed to the roll asperities ploughing deeper and sliding longer distance. Many more particles are formed when rough rolls are used, in agreement with the iron tape and reflection tape measurements. Moreover, it can be seen that the proportion of small wear particles is larger in the lubricated experiments than the dry ones. The two factors that may contribute to this difference are: (i) the difference in the predominant abrasive wear mode in lubricated and dry contact and (ii) the small wear particles can easily disperse in the oil in the lubricated experiments. Cutting is expected to be the dominant abrasive wear mechanism in the lubricated experiments and wedge forming in the dry ones (see Fig. 11). Cutting promotes formation

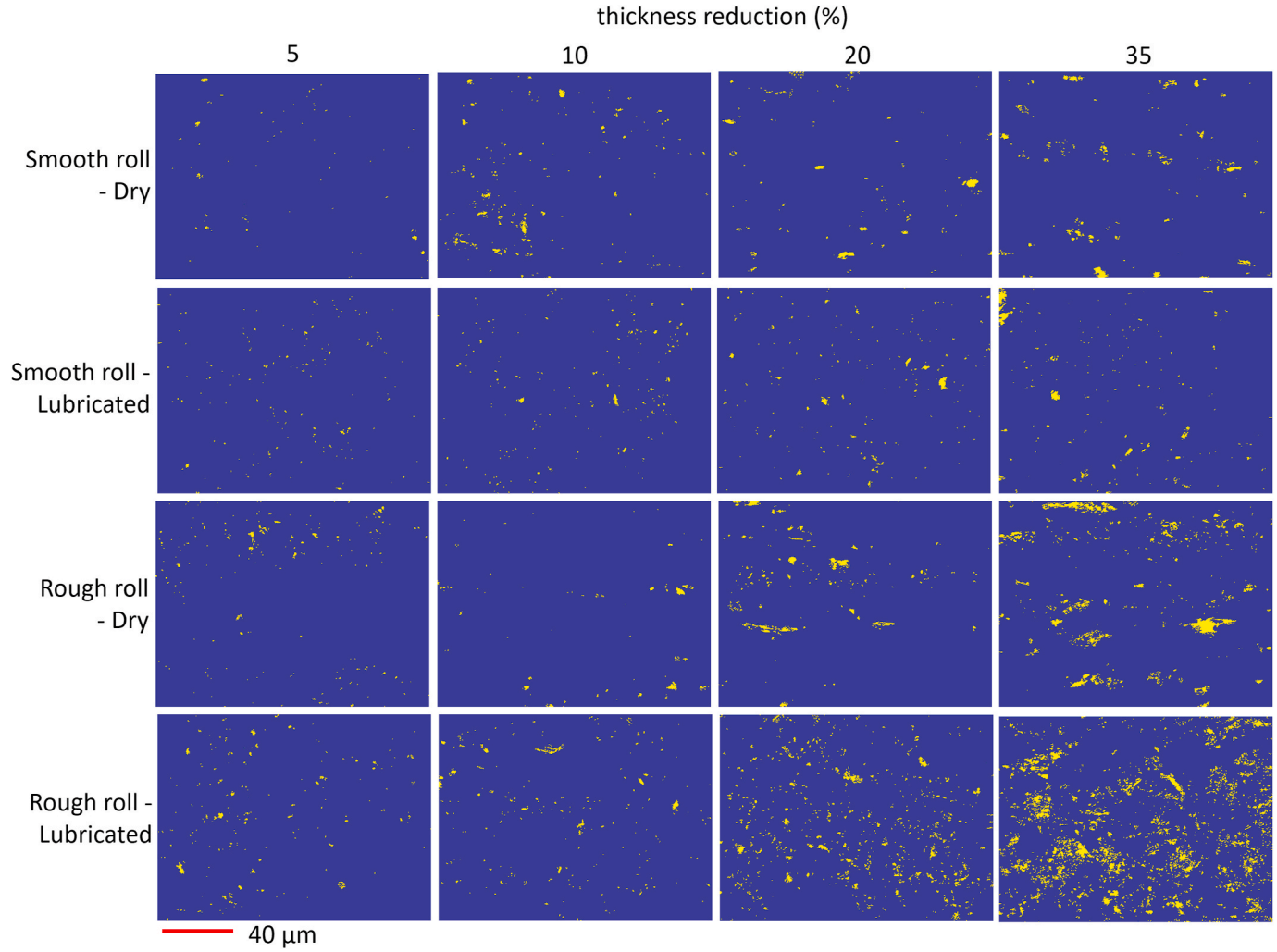

Fig. 19. The variation of wear particle distribution as a function of thickness reduction, roll roughness and lubrication.

of a small size flake-type wear particles [16]. Whereas, in wedge forming, wear debris are detached when the wedge growing ahead of the ploughing asperity reaches a critical size, see for example [29].

The statistical results of the size and quantity distribution of the wear particles is presented in Fig. 20. The microscopy images were taken at four different locations (for every rolling condition), each covering an area of 473 μm × 356 μm, to get a representative distribution of the particles. The size of the wear particles is defined by an equivalent diameter, which is the diameter of a circle with the same area as the particle. The wear particles with <5 μm in diameter constitute nearly 99% of the total number of wear particles and 80%–97% of the total area covered by wear particles. In contrast, particles bigger than 10 μm constitute only a very small fraction, less than 2% and 7% of the total area in the lubricated and dry experiments, respectively. The amount of big wear particles (>5 μm) increases with thickness reduction from about 5% of the total area at 5% thickness reduction to 19% at 35% thickness reduction. The roll asperities plough deeper into the strip surface and slide larger distance as the thickness reduction is increased, leading to the formation of bigger wear particles observed at high thickness reductions.

Fig. 21 compares the proportion of the surface area of the adhesive tape (strip) covered by wear particles. It exhibits good agreement with the iron tape measurements (Fig. 9). Less than 2% of the strip area is covered by wear particles when smooth rolls were used, irrespective of the thickness reduction. On the contrary, the wear particles cover an area as high as 7.5% of the strip surface at high thickness reduction when rough rolls were used under lubricated conditions.

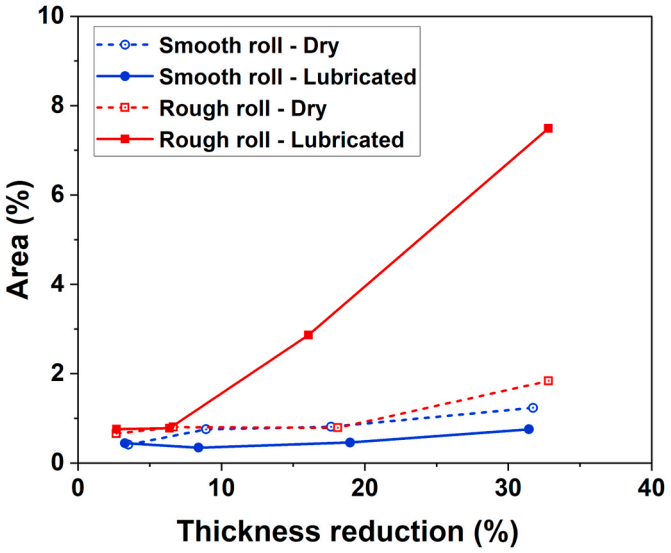

Fig. 21. The percentage area of the strip surface covered by wear particles.

4.2. Scratch experimental results

Modelling wear in cold rolling requires relating the influence of rolling parameters on the macroscale contact behavior and the microscopic wear mechanism at asperity level. The scratch experiments provide information about the microscopic wear mechanism and the volume of material removed as wear debris at single asperity contact.

The fraction of material removed (d_w) as a function of the degree of penetration (d_p) in the scratch experiments is graphed in Fig. 22. As expected, the degree of wear increases with increasing d_p. However, d_w starts to fluctuate heavily with increasing d_p. This is due to the high ductility of the material under investigation (Ti-IF steel), where the formed chips (sometimes) do not break off but remain next to the wear track, resulting in this fluctuation. Similar observation is reported in Ref. [17].

It is necessary to define the relationship between d_w and d_p in a mathematical equation to incorporate the scratch experiment results into the wear model (see section 2). Referring to Hokkirigawa et al. [30] experimental results obtained by sliding a spherical indenter on various

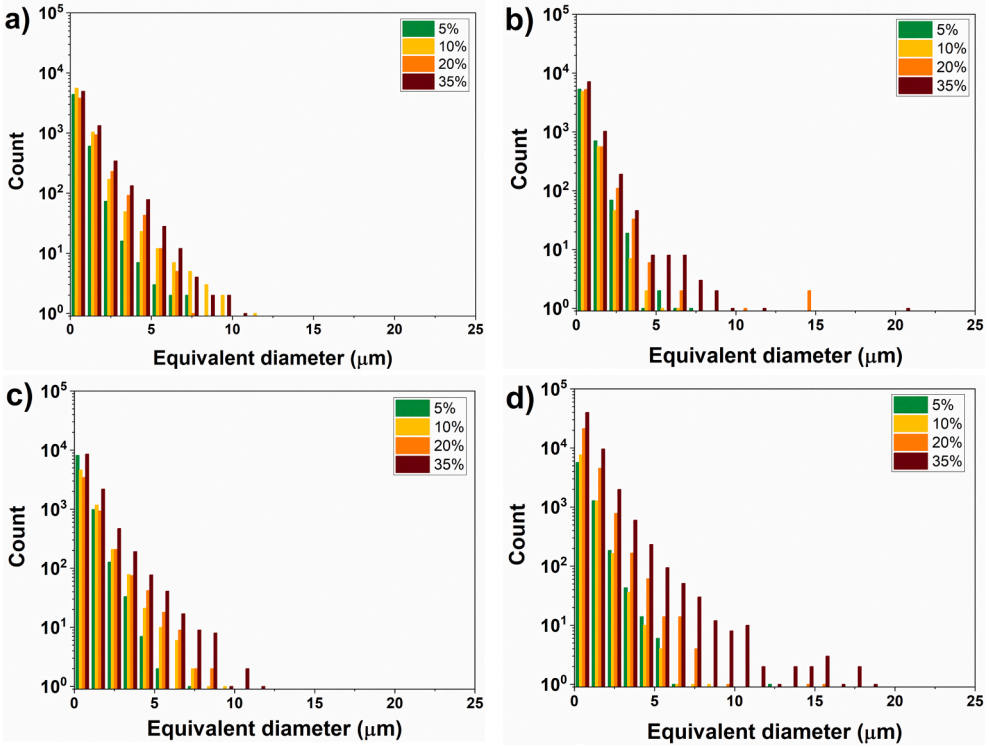

Fig. 20. Wear particle size distribution of the rolling experiments at several thickness reductions (5%, 10%, 20% & 35%): a) smooth roll – dry, b) smooth roll – lubricated, c) rough roll – dry, d) rough roll - lubricated.

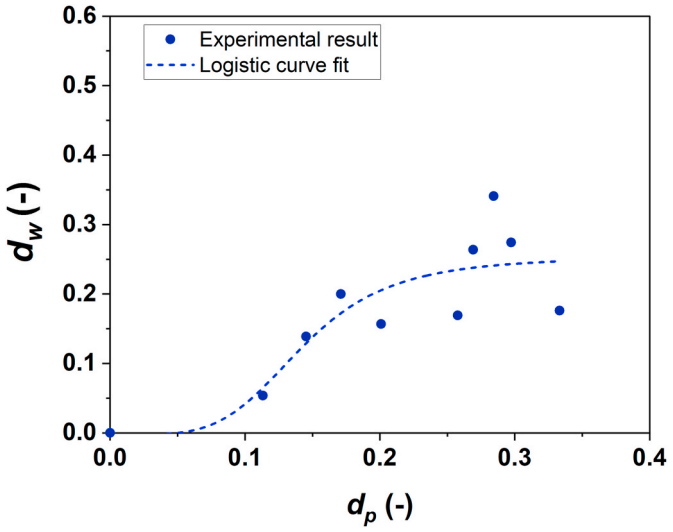

Fig. 22. Degree of wear as a function of degree of penetration.

heat treated steels, the degree of wear is expected to increase from 0 to a maximum value following an S-shaped curve, in which the maximum value depends on the material being scratched. Considering this, the experimental results are fitted by a logistic function, which has a characteristic S-shaped curve, following a least squared method curve fitting approach. The resulting equation is given by Eq. (9) and is plotted as a dashed line in Fig. 22.

$$d_w = 0.253 - 0.253 \Big/ \left(1 + \left(d_p/0.143\right)^{4.348}\right) \tag{9}$$

4.3. Model results

Comparison of the measured amount of wear and the model results for the lubricated rolling experiments are provided in Fig. 23. The model results presented here are an average of 18 simulations. Dissimilar surface roughness measurements (1.6 mm × 1.2 mm, lateral resolution 0.52 μm) of the roll and the strip were used for each simulation. The model results confirm that roll roughness and thickness reduction are the predominant rolling parameters that determine the amount of wear particles formation, rough roll and high thickness reduction giving the most wear. The observed higher wear when using rough rolls than smooth rolls is attributed to the higher d_p of asperities in the former.

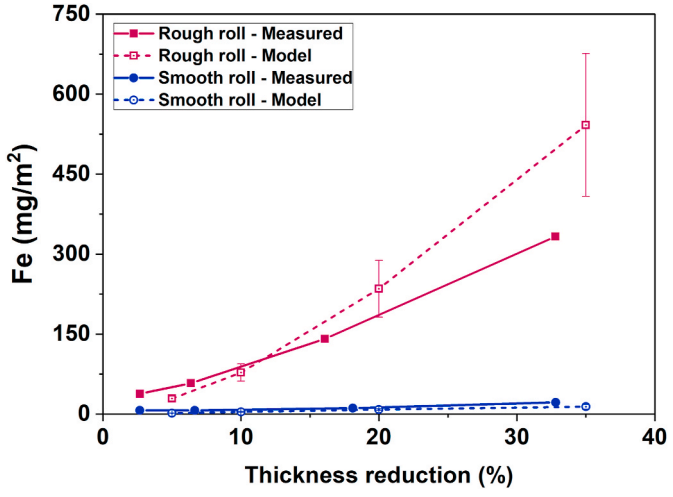

Fig. 23. Wear as a function of thickness reduction for the lubricated rolling experiments: Measured vs Model.

Fig. 24 illustrates an example of the d_p distribution at 20% thickness reduction for smooth and rough rolls. When smooth rolls are used, most asperity contacts will be in the ploughing regime and wear will occur only for relatively small number of asperity contacts which are sharp enough to operate in cutting or wedge forming wear mechanism. The high rate of wear particles formation at high thickness reductions is due to the increased severity of contact, i.e. the increased real area of contact and sliding distance at high thickness reduction. The high standard deviation of the model results suggests that the variation of the local roll roughness significantly influences the amount of wear. This can be, however, improved by utilizing surface roughness measurements covering a bigger area.

The model captures the trend correctly and give values in the same order of magnitude as the experiments. Nevertheless, noticeable differences are observed in terms of the exact amount of wear between the measured and the model results. The model underestimates the wear volume when using smooth rolls at all thickness reductions and at low thickness reductions when using rough rolls. Conversely, the model overestimates the wear volume when using rough rolls at high thickness reductions. In the current model, only abrasive wear is considered. Although abrasive wear can be regarded as the prime wear mechanism, it has to be emphasized that usually several wear mechanisms act simultaneously and the wear mechanisms interact. Adhesive, fatigue, corrosive and erosive wear are the potential other wear mechanisms may also contribute to wear in cold rolling operations [10]. Additionally, third body abrasive wear, caused by the hard oxide particles/hard phases like carbides from the strip which are broken away and dragged long the rolls also influence the mechanics, dynamics and chemistry of the sliding surfaces [32]. Plus, the scratch experiments were done for spherical asperities. However, the roughness asperities are irregular and this shape may affect the wear mechanism and the degree of wear. Kayaba et al. [33] studied the three dimensional shape effect on abrasive wear (both wear mode and wear rate) as a function of the attack angle and the dihedral angle. They showed that wear rate is sensitive to the change of both attack angle and dihedral angle. It has also to be noted that the influence of other rolling parameters such as roll diameter and lubricant temperature cannot be neglected as it affects the lubricant film thickness and performance of lubricant additives [5,8].

The slight underestimation of the wear volume by the model when using smooth rolls at all thickness reductions and at low thickness reductions when using rough rolls is most likely caused by the fact that hard oxide particles and carbides from the strip, which can break away, are not modelled. The overestimation of the model at high thickness reductions when using rough rolls is probably caused by the use of the real contact area at the exit of the roll bite, which is an overestimation of the actual real contact area. Another aspect of the varying relative speed throughout the roll bite is that a roll asperity that is directly behind the one ahead along the rolling direction will catch up and slide already created wear groove by the latter. This reduces the effective degree of penetration, and consequently, the wear volume. Besides, the degree of wear was measured in the scratch experiments for an ideal asperity, an approximate of the real shape of asperities.

In summary, the model covers the main physical phenomena related to wear particle generation and showed a good agreement with the experimental results. It can be developed further by including the influence of several other rolling parameters and influencing factors. For example, it can be extended for different material grades and cold rolling processes operating in the mixed lubrication regime.

5. Conclusion

Cold rolling experiments were conducted in dry and lubricated conditions at several thickness reductions, rolling speed and exit tension using smooth and rough rolls to investigate the effect of rolling parameters on the quantity of wear particles. Moreover, a wear model that combines macroscale contact model and wear at single asperity contact

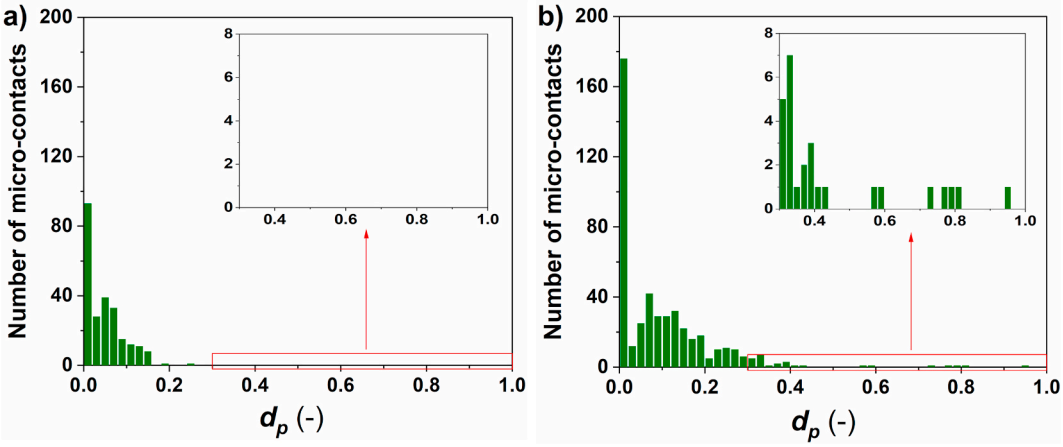

Fig. 24. The distribution of degree of penetration of roll asperities in contact with the strip at 20% thickness reduction for a) smooth roll and b) rough roll.

is proposed. Rolling experiments revealed that thickness reduction and roll roughness are the two dominant process parameters that control strip cleanliness/wear particles generation in cold rolling processes operating under boundary lubrication regime. The combination of rough rolls and high thickness reduction under lubricated contact resulted in the worst strip cleanliness. Rolling speed and exit tension (forward slip) exhibited little influence on strip cleanliness in the current experiments. Analysis of the wear particles size distribution showed that most of the wear particles are less than 5 μm (in diameter), constituting nearly 99% of the total number of the wear particles and 80%–97% of the total area covered by wear particles.

The proposed wear model covers the main physical phenomena related to wear particle generation. Furthermore, it captures the trend correctly and give values in the same order of magnitude as the experiments in terms of the volume of wear particles generated.

Credit author statement

M.A. Mekicha: Writing – original draft, Software, Visualization, Methodology. M.B. de Rooij: Conceptualization, Funding acquisition, Writing – review & editing. L.Jacobs: Resources, Investigation. D.T.A. Matthews: Writing – review & editing. D.J. Schipper: Supervision.

Declaration of competing interest

The authors declare that they have no known competing financial interests or personal relationships that could have appeared to influence the work reported in this paper.

Acknowledgements

This research was carried out under project number F41.1.14551 in the framework of the Partnership Program of the Materials innovation institute M2i (www.m2i.nl) and the Foundation of Fundamental Research on Matter (FOM) (www.fom.nl), which is part of the Netherlands Organization for Scientific Research (www.nwo.nl).

References

[1] Fisher TW, Iezzi RA, Madritch JM. Theoretical and practical considerations of sheet steel surface cleanliness. SAE Trans 1980;89:923–35. https://doi.org/10.2307/44632465.
[2] Pesci C, Monfort G, Torre V, Van Steden H, Kurzynski J, Vervaet B, et al. Controlling wear and surface cleanliness during cold rolling. (LOWWEAR); 2012. https://doi.org/10.2777/23177.
[3] Jacobs L, Vervaet B, Hermann H, Agostini M, Kurzynski J, Jonsson N-G, et al. Improving strip cleanliness after cold rolling. Proc Inst Mech Eng Part J J Eng Tribol 2011;225:959–69. https://doi.org/10.1177/1350650111413639.
[4] Januszkiewicz KR, Stratford G, Ward T. Roll bite conditions controlling formation of wear debris during cold rolling of aluminum. J Mater Process Technol 1994;45:117–24. https://doi.org/10.1016/0924-0136(94)90328-X.
[5] Labiapari W da S, de Alcântara CM, Costa HL, De Mello JDB. Wear debris generation during cold rolling of stainless steels. J Mater Process Technol 2015;223:164–70. https://doi.org/10.1016/J.JMATPROTEC.2015.03.050.
[6] Deltombe R, Dubar M, Dubois A, Dubar L. A new methodology to analyse iron fines during steel cold rolling processes. Wear 2003;254:211–21. https://doi.org/10.1016/S0043-1648(03)00005-X.
[7] Huart S, Dubar M, Deltombe R, Dubois A, Dubar L. Asperity deformation, lubricant trapping and iron fines formation mechanism in cold rolling processes. Wear 2004;257:471–80. https://doi.org/10.1016/J.WEAR.2004.01.012.
[8] Louaisil K, Dubar M, Deltombe R, Dubois A, Dubar L. Analysis of interface temperature, forward slip and lubricant influence on friction and wear in cold rolling. Wear 2009;266:119–28. https://doi.org/10.1016/J.WEAR.2008.06.003.
[9] Hui Z, Manxing W. A study of wear mechanisms in the cold rolling of aluminium strip. J Mater Process Technol 1992;31:235–43. https://doi.org/10.1016/0924-0136(92)90024-M.
[10] Turner CH. Tribology - understanding the cost of quality in cold rolling. Steel Times Iternational 1995;223:s6–7.
[11] Montmitonnet P, Delamare F, Rizoulieres B. Transfer layer and friction in cold metal strip rolling processes. Wear 2000;245:125–35. https://doi.org/10.1016/S0043-1648(00)00473-7.
[12] Montmitonnet P, Bouadjadja N, Luong LP, Bertrandie JJ, Dietsch H. On the mechanism by which chromium improves strip surface cleanliness in steel strip cold rolling. Key Eng Mater 2018;767:240–7. https://doi.org/10.4028/www.scientific.net/KEM.767.240.
[13] Wilson WRD, Walowit JA. An isothermal hydrodynamic lubrication theory for strip rolling with front and back tension. J Lubr Technol 1971;92:69–74.
[14] Mekicha MA, de Rooij MB, Jacobs L, Matthews DTA, Schipper DJ. Experimental validation of contact models for cold-rolling processes. J Mater Process Technol 2020;275:116371. https://doi.org/10.1016/j.jmatprotec.2019.116371.
[15] Dieter GE, Bacon DJ. Mechanical metallurgy. London: McGraw-Hill; 1988.
[16] Hokkirigawa K, Kato K. An experimental and theoretical investigation of ploughing, cutting and wedge formation during abrasive wear. Tribol Int 1988;21:51–7. https://doi.org/10.1016/0301-679X(88)90128-4.
[17] Masen MA, de Rooij MB, Schipper DJ. Micro-contact based modelling of abrasive wear. Wear 2005;258:339–48. https://doi.org/10.1016/J.WEAR.2004.09.009.
[18] Masen MA, de Rooij MB. Abrasive wear between rough surfaces in deep drawing. Wear 2004;256:639–46. https://doi.org/10.1016/j.wear.2003.10.006.
[19] Wilson WRD, Sheu S. Real area of contact and boundary friction in metal forming. Int J Mech Sci 1988;30:475–89. https://doi.org/10.1016/0020-7403(88)90002-1.
[20] Lenard JG. Metal forming science and practice. Elsevier; 2002. https://doi.org/10.1016/b978-0-08-044024-8.x5000-0.
[21] Azushima A, Yoneyama S, Yamaguchi T, Kudo H. Direct observation of microcontact behavior at the interface between tool and workpiece in lubricated upsetting. CIRP Ann - Manuf Technol 1996;45:205–10. https://doi.org/10.1016/S0007-8506(07)63048-0.
[22] Azushima A, Uda M, Kudo H. An interpretation of the speed dependence of the coefficient of friction under the micro-PHL condition in sheet drawing. CIRP Ann - Manuf Technol 1991;40:227–30. https://doi.org/10.1016/S0007-8506(07)61974-X.
[23] Bay N, Bech JI, Andreasen JL, Shimizu I. Studies on micro plasto hydrodymic lubrication in metal forming. Met. Form. Sci. Pract. A state-of-the-Art Vol. Honor. Prof. J.A. Schey 2002:115–34 [Chapter 7]., Elsevier.
[24] Bech J, Bay N, Eriksen M. Entrapment and escape of liquid lubricant in metal forming. Wear 1999;232:134–9. https://doi.org/10.1016/S0043-1648(99)00136-2.
[25] Patir N, Cheng HS. An average flow model for determining effects of threedimensional roughness on partial hydrodynamic lubrication. J Tribol 1978;100:12–7. https://doi.org/10.1115/1.3453103.

[26] Tabor D. Junction growth in metallic friction: the role of combined stresses and surface contamination. Proc R Soc London Ser A Math Phys Sci 1959;251:378–93. https://doi.org/10.1098/rspa.1959.0114.
[27] Gåård A, Sarih RM. Influence of tool material and surface roughness on galling resistance in sliding against austenitic stainless steel. Tribol Lett 2012;46:179–85. https://doi.org/10.1007/s11249-012-9934-7.
[28] Mizuno T, Hasegawa K. Effects of die surface roughness on lubricating conditions in the sheet metal compression-friction test. J Tribol 1982;104:23–8. https://doi.org/10.1115/1.3253160.
[29] Kayaba T, Hokkirigawa K, Kato K. Analysis of the abrasive wear mechanism by successive observations of wear processes in a scanning electron microscope. Wear 1986;110:419–30. https://doi.org/10.1016/0043-1648(86)90115-8.
[30] Hokkirigawa K, Kato K, Li ZZ. The effect of hardness on the transition of the abrasive wear mechanism of steels. Wear 1988;123:241–51. https://doi.org/10.1016/0043-1648(88)90102-0.
[31] Lenard JG. Primer on flat rolling. second ed. Elsevier; 2014. https://doi.org/10.1016/C2012-0-06474-5.
[32] Gonçalves JL, de Mello JDB, Costa HL. Wear in cold rolling milling rolls: a methodological approach. Wear 2019;426–427:1523–35. https://doi.org/10.1016/j.wear.2018.12.005.
[33] Kato K, Hokkirigawa K, Kayaba T, Endo Y. Three dimensional shape effect on abrasive wear. J Tribol 1986;108:346–9. https://doi.org/10.1115/1.3261193.